Engineered Science
DOI: https://dx.doi.org/10.30919/es1846

Influence of Relay Chimney Design Parameters on Indoor Natural Smoke Exhaust Characteristics for Shanpian Dwelling: Numerical Simulation Study

Yunke Yang,[1] Xiaoliang Wang,[1,2,*] Guanxing Pu,[1] Junjia Hu,[1] Shuliang Li,[1,2] Li Yang[1,2] and Xianmin Mai[1,*]

Abstract

The Shanpian dwelling (SD), a traditional vernacular architecture in Northwest Yunnan, China, produces continuous smoke during domestic fire use due to open combustion, and the smoke is discharged through the chimney above the open firepit. However, the quantitative relationship between chimney dimensions and smoke extraction efficiency remains underexplored in existing research. This paper establishes a computational fluid dynamic (CFD) based numerical model for SD smoke flow, systematically investigating the impact of chimney design parameters on air changes per hour (ACH, h^{-1}), indoor carbon dioxide concentration (ICDC, ppm), smoke extraction velocity rate (SEVR, m/s) and indoor average temperature of 1.5 m (IAT of 1.5 m, ℃). Results demonstrate that enlarging the chimney sectional area substantially enhances ACH (peaking at 54.97 h^{-1}), yet exerts a negligible influence on flue gas velocity (the change amount is less than 0.25 m/s), suggesting air quality improvement primarily through volumetric flow augmentation rather than velocity elevation. The influence of the length and width of the chimney section on each evaluation index has a critical point (length is 0.75 m, width is 0.55 m). When the length or width of the section is lower than the critical point, its influence on each index is more significant. However, when it exceeds the critical point, its influence on each index gradually slows down. This paper summarizes the smoke flow patterns in SD, points out the linear relationship between indoor air quality and chimney area, and proposes an optimization suggestion that the chimney size should be larger than the firepit section, providing a scientific basis for the ventilation design of traditional dwellings.

Keywords: Shanpian dwelling; Natural smoke extraction; Indoor air quality; Numerical simulation; Chimney design parameters.

Received: 06 June 2025; Revised: 23 October 2025; Accepted: 29 October 2025.
Article type: Research article.

1. Introduction

As carriers of regional culture and ecological wisdom, the architectural forms and environmental adaptation strategies of traditional dwellings have always been important topics in architectural and ecological studies. The Shanpian dwelling (SD) in Shangri-La is a typical representative of traditional settlements on the Qinghai-Tibet Plateau. Its core space, the firepit, not only serves as the functional center for heating and cooking in daily life, but also carries significant social meanings such as family gatherings, cultural inheritance, and ritual activities, thus becoming a spiritual symbol that sustains community identity.[1,2] However, the long-term burning of biomass fuels like wood and cow dung in the firepit can easily produce pollutants, such as Carbon Monoxide and Carbon Dioxide (CO and CO_2),[3,4] which may affect the health of the residents. To enhance the natural ventilation effect in the SD, after long-term practical exploration, the SD have developed a unique structure named Relay Chimney. That is, a vertical wooden chimney extending above the firepit connects with the attic space to form a continuous airflow channel. The natural ventilation is achieved by utilizing the thermal pressure generated by the firepit combustion. This structure is different from the traditional design where the chimney is directly connected to the furnace. It not only achieves the physical isolation of smoke and the indoor environment through the ingenious organization of the building space, but also avoids

[1] *School of Architecture, Southwest Minzu University, Chengdu, 610225, China*
[2] *Institute of Qinghai-Tibetan Plateau, Southwest Minzu University, Chengdu, 610225, China*
**E-mail*: xiao_liangwang@126.com (X. Wang);
maixianmin@foxmail.com (X. Mai)

the energy consumption issues of modern mechanical ventilation systems. Thus, it ensures that a good indoor air quality can still be maintained in high-altitude and low-oxygen environment,[5,6] demonstrating the ecological wisdom of regional architecture.[7] Furthermore, the Relay Chimney retains the open exhaust method, ensuring that the indoor wood is protected from insect damage after being exposed to smoke. Field monitoring has shown that this system can control the indoor CO_2 concentration within a safe range of 450-480 ppm, making the indoor CO_2 concentration close to that of the outdoor, which is significantly superior to that of ordinary residences.[8,9] Therefore, it is necessary to deeply explore the smoke exhaust characteristics and smoke flow patterns of this relay smoke exhaust system in traditional dwellings, in order to provide technical support for the renewal and renovation of traditional dwellings in the new era.

In recent years, scholars' studies on pollutants in traditional dwellings or natural ventilation has mainly focused on the emission characteristics of pollutants from firepits,[10,11] qualitative descriptions of ventilation optimization,[12,13] or simulations of chimney effects in modern buildings,[14,15] and has formed a multi-dimensional methodological framework. By combining on-site monitoring with computational fluid dynamic (CFD) simulation, the pollutant diffusion laws for different fuel types were revealed;[16-21] thermal evaluation indicators for traditional Chinese Kang were constructed (such as surface temperature and thermal inertia),[22-28] providing a quantitative tool for indoor environmental assessment; for the simulation of smoke flow in high-rise and large-span buildings,[29,30] a simulation method for fire smoke fluid dynamics was developed. Although these achievements did not directly conduct research on the relay smoke exhaust system, and lacked quantitative studies on the geometric design parameters (such as cross-sectional dimensions and height-width ratio) of the relay chimney in high-altitude and large temperature difference environments, the research ideas and methods they involved can provide strong technical support and reference ideas for this study. Therefore, it is necessary to conduct a scientific and depth analysis of the internal mechanism of natural smoke exhaust through the relay chimney in the low-pressure and large temperature difference environment of the Qinghai-Tibet Plateau.[16-20]

Based on this, this study takes the relay chimney in SD as the research object. By establishing a CFD numerical model, it systematically analyzes the influence mechanisms of chimney design parameters such as cross-sectional size and height-width ratio on air changes per hour (ACH, h^{-1}), indoor carbon dioxide concentration (ICDC, ppm), smoke extraction velocity rate (SEVR, m/s) and indoor average temperature of 1.5 m (IAT of 1.5 m, ℃). The research aims to reveal the natural smoke exhaust mechanism of the relay chimney, quantify its improvement effect on indoor air quality, clarify the optimization thresholds of key design parameters, explore the ecological value of traditional building passive technologies, and provide a scientific basis for the renewal, renovation, and protection and utilization of traditional dwellings.

2. Research object and methods

2.1 Research object

This research focuses on the natural smoke extraction efficacy of residential firepits in the traditional SD located in Shangri-La (Fig S1), Diqing Tibetan Autonomous Prefecture, Yunnan Province in China. The SD is a unique traditional residential form in this area. Its architectural structure is mostly made of earth and wood or stone and wood, featuring compact interior spaces and limited ventilation conditions. While fulfilling essential living requirements, this architectural typology concurrently contends with the Indoor Air Quality (IAQ) deterioration and health risks from prolonged biomass combustion.

2.1.1 Geography and climate environment

The research site is located in the Shangri-La area in the northwest of Yunnan Province, at 28.00 °N latitude and 99.55 °E longitude. The terrain of this area is complex, and the climate is diverse. At a mean altitude of 3,276 m, the hypoxic atmosphere combines with intense solar radiation and significant diurnal temperature variation, resulting in indoor and outdoor temperature differentials exceeding 8.00 ℃ during winter. These climate challenges drive architectural adaptations prioritizing thermal retention and wind resistance, resulting in constrained ventilation apertures that exacerbate smoke accumulation. This means that a larger chimney will be required.

2.1.2 Building features of SD

The case study examines a 150-year-old SD (Fig. 1) comprising a three-story structure (excluding attic space) with a total height of about 8.50 m, located in a preserved village cluster 36 km northwest of Shangri-La urban center. Functionally, the ground floor serves as livestock quarters, while the upper floors contain residential spaces. The second-floor main chamber (2.75 m clear height) houses the central firepit at its southwest quadrant, connected via a vertically integrated chimney flue to the outer space, the geometric model is illustrated in Fig. 2. The thermal stack vertically extends 2.65 m through the third floor with sectional

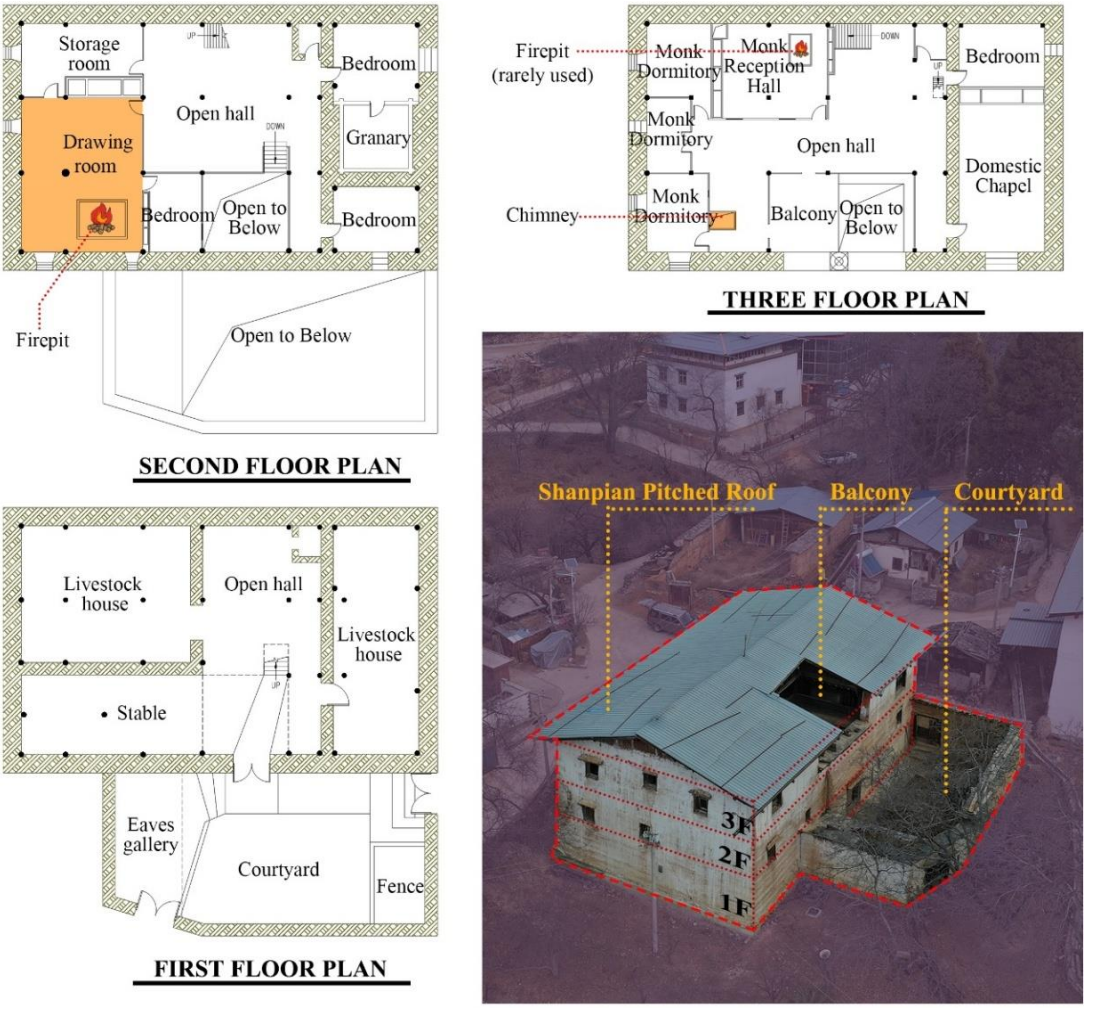

Fig. 1: Current status of the building and floor plan.

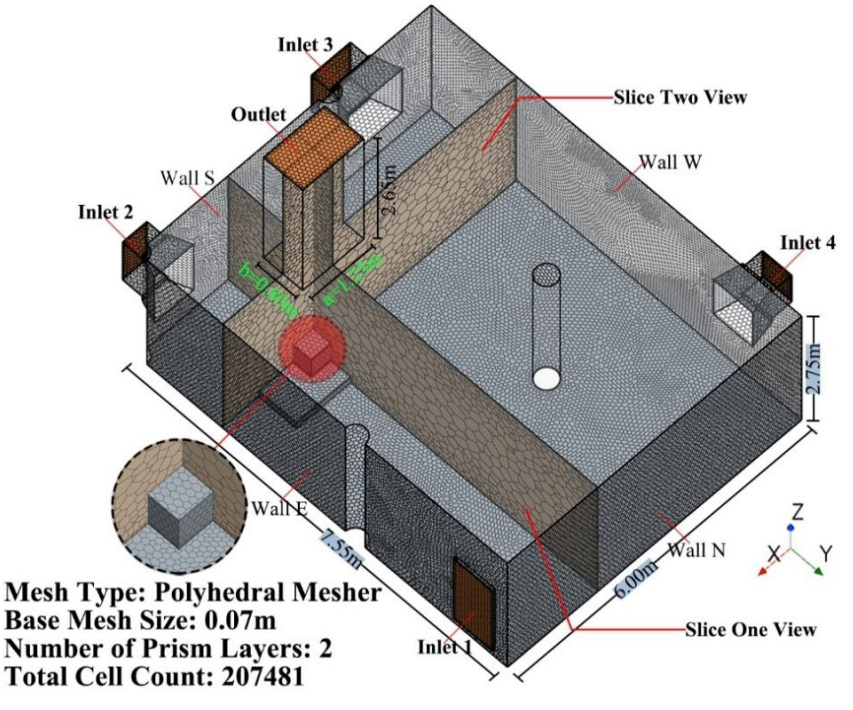

Fig. 2: Model and grid schematic diagram.

Table 1: The dimensions of the door and window openings in the living room.

Opening location	Designation	Opening dimensions L(m)×W(m)	Hole area (m^2)
East door	Inlet 1	1.60×0.80	1.28
Southeast window	Inlet 2	1.00×0.50	0.50
Southwest window	Inlet 3	0.95×0.80	0.76
West window	Inlet 4	0.70×0.60	0.42

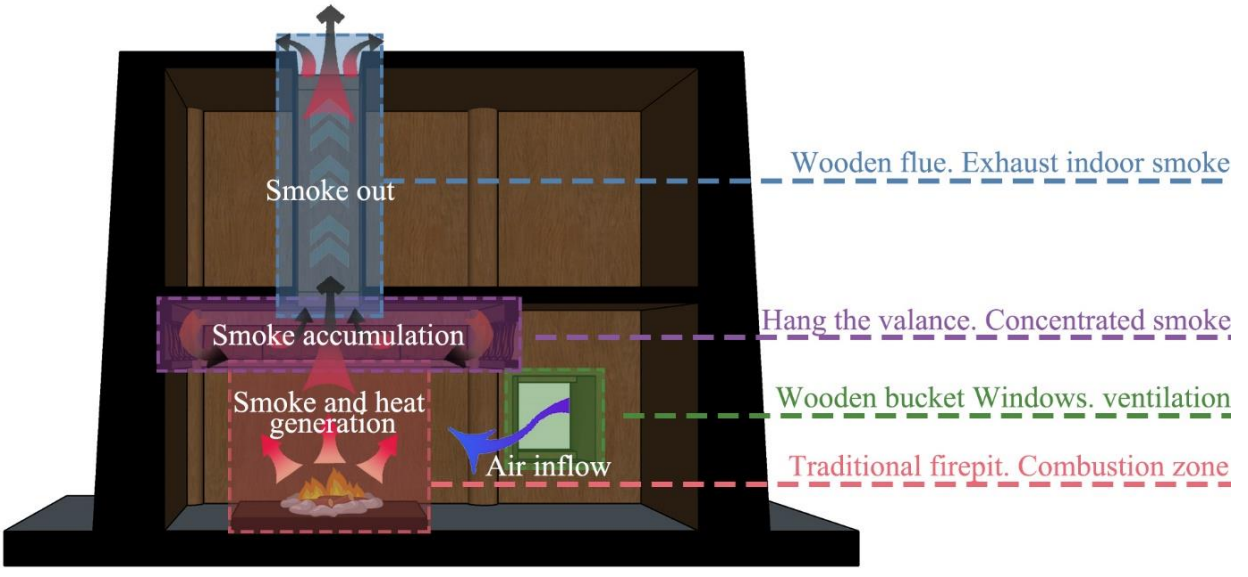

Fig. 3: Schematic diagram of the open relay firepit smoke exhaust system in the SD.

dimensions 1.25 m (L) × 0.80 m (W), exhibiting aspect ratio 1.56 and sustaining buoyancy driven transport. The room has four openings to the outside, including a door on the east side, two windows on the south side, and one window on the west side. The specific dimensions are shown in Table 1.

2.1.3 Firepit and natural smoke exhaust

The firepit system in the SD is the core area of residents' life, located in the main house on the second floor. The firepit is an open structure, and the main fuel is dry firewood collected by residents in the mountain valleys. Since the firepit is never extinguished throughout the year, a large amount of smoke is produced during the burning process, leading to a decline in IAQ. As seen in Fig. 3, the firepit and natural smoke exhaust system include the hanging valance, wooden door and window openings, and the wooden relay chimney. Smoke evacuation primarily relies on vertical stack effects, where chimney geometry and dimensional parameters critically govern extraction efficiency through thermal draft mechanisms. This study analyzed the indoor smoke flow characteristics and their impact on air quality under different chimney scales through a combination of numerical simulation and field testing, aiming to provide a scientific basis for the optimization of the exhaust system in the traditional SD.

Architecturally, the 2.65 m vertical chimney stack integrated with the attic space constitutes a natural draft pathway. The second-floor chamber contains four openings creating constrained ventilation regimes. The research particularly focuses on the influence of the special climatic conditions at high altitudes on the buoyancy of smoke, and the temperature during the operation above the firepit is obtained through on-site measurement.

2.2 Research methods

This study employs a validated CFD framework to systematically investigate the dynamics of smoke transport related to chimney design parameters and associated IAQ impacts in the SD. The following is a detailed numerical simulation research method, including model and assumptions, control equations, boundary conditions, and physical parameters, as well as fire source settings and other contents.

2.2.1 Models and assumptions

To accurately simulate the indoor smoke flow in the SD, this study established a numerical simulation model of indoor smoke flow. The model is based on the following assumptions:

(1) Simplify the building model: the core objective of the research is to analyze the influence of chimney design parameter changes on flue gas flow rather than the overall layout of the building. Moreover, the main house on the second floor is the core functional area where the firepit is located, and the flue gas pollution problem is the most significant. The doors of other rooms and the main house are always closed and have no direct connection with the chimney. Therefore, only the main house on the second floor and the chimney are modeled, and the influence of other rooms is ignored. The main internal structures of the main house include walls, floors, doors and windows, columns, valance, and chimneys. All these structures have already been constructed in the model.

(2) The thermal properties of materials are consistent: as the flue gas flow is mainly driven by buoyancy effect (thermal convection) and pressure gradient, the influence of the thermal properties of the materials on the gas flow pattern is much smaller than that of temperature difference and geometric structure. Unifying the material parameters can avoid the interference of secondary factors in the sensitivity analysis of the main variable (chimney design parameters). Therefore, it is assumed that the thermal properties of the exterior wall and floor materials are the same, and their influence on flue gas flow is ignored.

(3) Neglecting radiative heat transfer: the temperature of the flue gas produced by the combustion in the firepit is usually between 100 ℃ and 300 ℃, and its flow is mainly driven by natural convection due to thermal buoyancy. According to Stefan-Boltzmann's law, the intensity of radiative heat transfer is proportional to the fourth power of the temperature. In this temperature range, the radiative heat flux is much lower than the dominant effect of convection. Furthermore, through the trial calculation of three groups of models with different chimney cross-sectional dimensions, it was found that the mean values of the selected indicators changed within 2 % before and after the addition of the radiation model (Table 2, + indicates the addition of radiation model in first column). In this study, we only focus on the average conditions of each parameter indoors, so to improve the calculation efficiency, the radiation model will not be added in the subsequent calculations.

(4) Fix the sizes and positions of the door and window openings: do not discuss the sizes and positions of the door and window openings, but only study the influence of the changes in the chimney size on the flow of flue gas.

2.2.2 Control equations

The research was conducted using the Fire and Smoke Wizard modular model, and the turbulence model adopted was the Realizable K-ε model. Since flue gas pollutants are not tracked in this paper, the component transport model is not used. Throughout the entire calculation process, the indoor smoke flow process conformed to the conservation equations of mass, energy, and momentum.[24-31]

The continuity Eq. (1):

$$\frac{\partial \rho}{\partial t}+\frac{\partial(\rho u)}{\partial x}+\frac{\partial(\rho v)}{\partial y}+\frac{\partial(\rho w)}{\partial z}=0 \quad (1)$$

where ρ is instantaneous value of the density of the gaseous mixture, kg/m³; u is the velocity of flue gas in the x-direction, m/s; v is the velocity of flue gas in the y-direction, m/s; w is the velocity of flue gas in the z-direction, m/s.

The energy conservation Eq. (2):

$$\frac{\partial(\rho c_p T)}{\partial t}+\nabla\cdot\left(\rho c_p v T\right)=\nabla\cdot(k\nabla T)+S_h+q_w \quad (2)$$

where c_p is constant pressure specific heat capacity, J/(kg·K); T is flue gas temperature, K; v is flue gas velocity vector, m/s;

Table 2: Comparison of results before and after adding the radiation model.

Model name	ACH (h^{-1})	Rate of change (%)	SEVR (m/s)	Rate of change (%)	ICDC (ppm)	Rate of change (%)	IAT of 1.5m (℃)	Rate of change (%)
Model 1	22.47	-0.86	1.37	-0.84	480.64	1.49	7.69	1.60
Model 1 +	22.28		1.36		487.80		7.82	
Model 2	35.41	-0.10	1.30	-0.08	461.94	0.04	7.65	-0.05
Model 2 +	35.44		1.30		462.14		7.59	
Model 3	14.06	-0.15	1.44	-0.18	524.49	1.06	8.59	-1.20
Model 3 +	14.04		1.43		530.05		8.49	

k is the thermal conductivity of the gaseous mixture, W/(m·K); S_h is the heat source item for the firepit combustion, W/m^3; q_w is wall heat transfer rate, W/m^3.

The momentum conservation Eqs. (3)-(5):

$$\frac{\partial(\rho u)}{\partial t}+\frac{\partial(\rho uu)}{\partial x}+\frac{\partial(\rho uv)}{\partial y}+\frac{\partial(\rho uw)}{\partial z}=(\frac{\partial\tau_{xx}}{\partial x}+\frac{\partial\tau_{xy}}{\partial y}+\frac{\partial\tau_{xz}}{\partial z})-\frac{\partial p}{\partial x} \quad (3)$$

$$\frac{\partial(\rho v)}{\partial t}+\frac{\partial(\rho vu)}{\partial x}+\frac{\partial(\rho vv)}{\partial y}+\frac{\partial(\rho vw)}{\partial z}=(\frac{\partial\tau_{yx}}{\partial x}+\frac{\partial\tau_{yy}}{\partial y}+\frac{\partial\tau_{yz}}{\partial z})-\frac{\partial p}{\partial y} \quad (4)$$

$$\frac{\partial(\rho w)}{\partial t}+\frac{\partial(\rho wu)}{\partial x}+\frac{\partial(\rho wv)}{\partial y}+\frac{\partial(\rho ww)}{\partial z}=\left(\frac{\partial\tau_{zx}}{\partial x}+\frac{\partial\tau_{zy}}{\partial y}+\frac{\partial\tau_{zz}}{\partial z}\right)-\frac{\partial p}{\partial z}+(\rho_{air}-\rho)g \quad (5)$$

where t is time, s; ρ_{air} is the local ambient air density, kg/m^3; μ is dynamic viscosity, Pa·s; τ is viscous stress tensor component; p is the local ambient atmospheric pressure, Pa; g is gravitational acceleration vector, m/s^2.

2.2.3 Boundary conditions and physical property parameters

(1) Boundary conditions

Outlet conditions: the chimney and door, and window outlets adopt pressure outlets, and the outlet gauge pressure is set to zero.

Indoor wall and floor conditions: the indoor wall and floor conditions adopt no-slip conditions. Since the altitude is about 3000 m, the heat transfer coefficient between the flue gas and the inner surface of the wall is set at 8.0 W/m^2·K.[32]

Interface conditions: the contact surface between the firepit and the indoor space is set as an interface to ensure heat exchange.

(2) Physical property parameter

The subject of this study is located in the Qinghai-Tibet Plateau region. The air conditions in high-altitude areas differ significantly from those in low-altitude areas. Therefore, after calculation, the physical parameters of the air are set in Table 3.

2.2.4 Fire source setting

The t^2 fire model is adopted to simulate the combustion of the firepit and can be used to represent the combustion situation of the firepit.[31] The heat release rate of the heat source of the firepit develops according to the t^2 law of time, and its growth curve can be represented by Eq. (6):

$$Q=\alpha t^2 \quad (6)$$

where Q is the heat release rate, kW, the maximum heat release rate is 3.50 kW when the fire reaches to steady status; α is the growth coefficient, kW/s^2, 3.0 kW/s^2 in this study; t is the burning time of the fire source, s.

2.3 Comparison of experimental and simulation results

2.3.1 Experimental conditions

(1) Experimental objective

To validate the accuracy of the subsequent CFD calculations, we conducted a field experiment. We carried out a combustion experiment in a well-preserved SD in Shangri-La City, as shown in Fig. 2. The experiment recorded the temperature inside the chimney and the carbon dioxide concentration in the room during the firepit combustion, which was used for subsequent simulation validation. The experiment recorded the temperature inside the chimney and the carbon dioxide concentration in the room during the firepit combustion, which was used for subsequent simulation validation.

(2) Experimental content and instrument arrangement

The instruments used in the experiment are listed in Table 4. The Thermocouple probe used in the experiment was suspended at different heights inside the chimney to set up four measurement points, as shown in Table 5. During the process of the flue gas being discharged from the chimney, the temperature values of each measurement point were automatically recorded every five minutes through the automatic recording function of the Four-channel temperature recorder. Additionally, the humidity and temperature recorder and the carbon dioxide detector were manually recorded to read the outdoor temperature and humidity conditions and the indoor carbon dioxide concentration every five minutes. Moreover, the test values under different combinations of window and door openings were recorded, and each opening combination was tested for 10 to 15 minutes.

2.3.2 Validation status

To ensure the reliability and accuracy of the numerical simulation results, this study validate the numerical model through the following methods:

(1) Due to the different combinations of opening and closing of the various holes, after one experiment is completed, before starting the next one, fuel needs to be added, and the doors and windows need to be manually opened or closed. Therefore, manual recording will have the characteristic of time mismatch compared to automatic recording. Therefore, when taking values for the automatic recording instrument, it takes the readings of the manual recording period and the readings 5 minutes before and after this period (a total of 5-6 values). After data processing, it is then validated against the simulation.

(2) Data processing: due to fluctuations during the

Table 3: Air physical property parameter value.

Density (kg/m^3)	Atmosphere (Pa)	Specific heat capacity (J/kg·K)	Thermal conductivity (W/(m·K))	Dynamic viscosity ($\times 10^{-5}$ Pa·s)	Prandtl number
0.88	68450.00	1004.96	0.024	1.71	0.71

Table 4: Experimental instruments.

Instrument name	Instrument picture	Instrument model	Measurement content	Range	Precision
Humidity and Temperature Recorder		Testo 174H	Record the indoor air temperature and relative humidity under non-burning conditions	-20 ℃~70 ℃ 2%~98%	±0.5 ℃
Four-channel temperature recorder		Testo 176T4	The temperature of the smoke at different heights above the fire pit	-200 ℃~1000 ℃	±0.3 ℃
Thermocouple probe		TT-K-30 SMPW			
Carbon dioxide detector		CEM DT802	Indoor CO_2 concentration monitoring	0~9999 ppm	±75 ppm

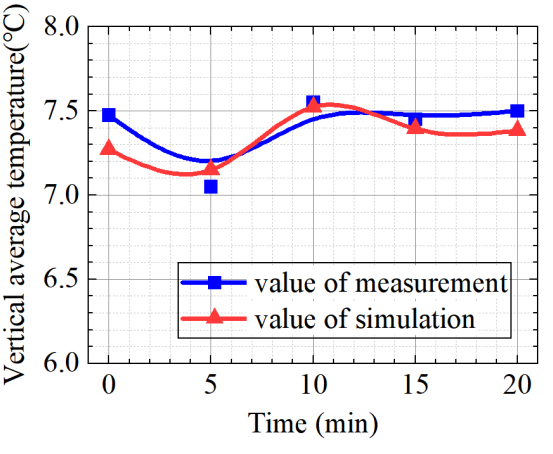

Fig. 4: Validation chart of average temperature above the chimney.

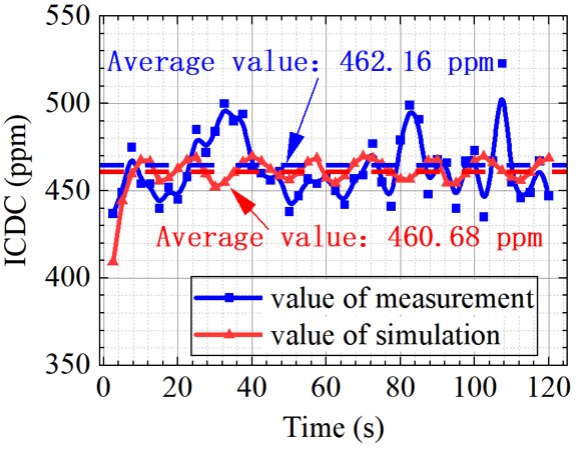

Fig. 5: Validation chart of indoor carbon dioxide concentration.

combustion process, there are sudden changes in the measured values. In order to improve the reliability of the data, after removing the abrupt values, the average value of the four vertical points in the chimney at different times was taken as the experimental result.

(3) Comparative analysis: the average temperature above the firepit under fully open doors and windows within twenty minutes obtained from the simulation was compared with the experimental measurement values (Fig. 4).

(4) The on-site records the changes in indoor carbon dioxide concentration during the experiment. We further validated the simulation. Due to the combination of various opening methods of doors and windows and the influence of the outdoor wind field, the fluctuation of the recorded values in the experiment was more significant. However, in Fig. 5, the average state was basically consistent with the simulation results, which validated the reliability of the calculation.

The validation results show that the simulated values are very close to the measured values, validated the accuracy of the numerical model.

2.4 Evaluation index

To comprehensively evaluate the changes in indoor flue gas flow and air quality in the SD under different chimney scales, the following evaluation indicators were selected in this study:

(1) Air changes per hour (ACH, h^{-1})

The IAQ is evaluated by calculating the ACH of the room. In the software, the mass flow rate of door and window openings and smoke outlets can be obtained. Through calculate by Eq. (7), the ACH of the outlet room can be determined.[33]

$$n = \frac{Q}{\rho V} \times 3600 \quad (7)$$

where n is ACH, h^{-1}; Q is ventilation quantity, kg/s; V is room volume, 126.55 m^3; ρ is air density, 0.88 kg/m^3.

During the on-site experiment, under the condition of natural ventilation with all doors and Windows fully open, the ACH of this type of building can reach up to 30.32 h^{-1} at most.

(2) Smoke extraction velocity rate (SEVR, m/s)

It refers to the average rate at which flue gas flows through the outlet plane of the chimney within a unit of time. If the flow rate is too fast, it will lead to faster combustion and high energy consumption. Too slow smoke exhaust rate will cause indoor smoke to accumulate in a short period of time, seriously affecting the life and health of residents.

(3) Indoor carbon dioxide concentration (ICDC, ppm)

It refers to the indoor carbon dioxide concentration. The Fire and Smoke Wizard modular model by default, uses passive scalar simulation to model the smoke flow, and the field function provides the smoke density function. By extracting the carbon smoke density value, the indoor carbon dioxide concentration is converted. Therefore, the indoor air conditions under several working conditions can be analyzed based on the average indoor carbon dioxide concentration.

(4) Indoor average temperature of 1.5 m (IAT of 1.5 m, ℃)

Due to the influence of flue gas temperature, a faster flue gas discharge rate may cause changes in indoor temperature. Therefore, the average indoor temperature at a height of 1.5 m is selected as the evaluation index, and combined with the flue gas discharge rate at the outlet, the quality of the chimney can be evaluated.

3. Results and discussion

3.1 Research on the flow law of indoor flue gas

Through numerical simulation, the flow characteristics of natural indoor smoke exhaust in the SD under different chimney parameters were studied, which are specifically manifested as:

(1) Dynamic characteristics of flue gas flow: as shown in Fig. 6, within 300 s of operation in the firepit, in addition to

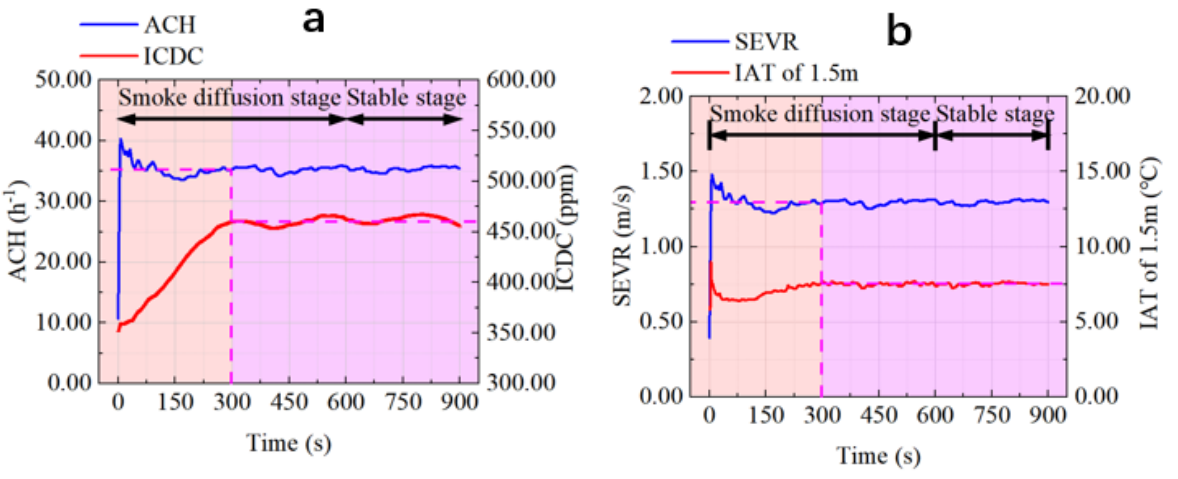

Fig. 6: The changes of various parameters indoors after the firepit has been running for 300 s, (a) ACH and ICDC; (b) SEVR and IAT.

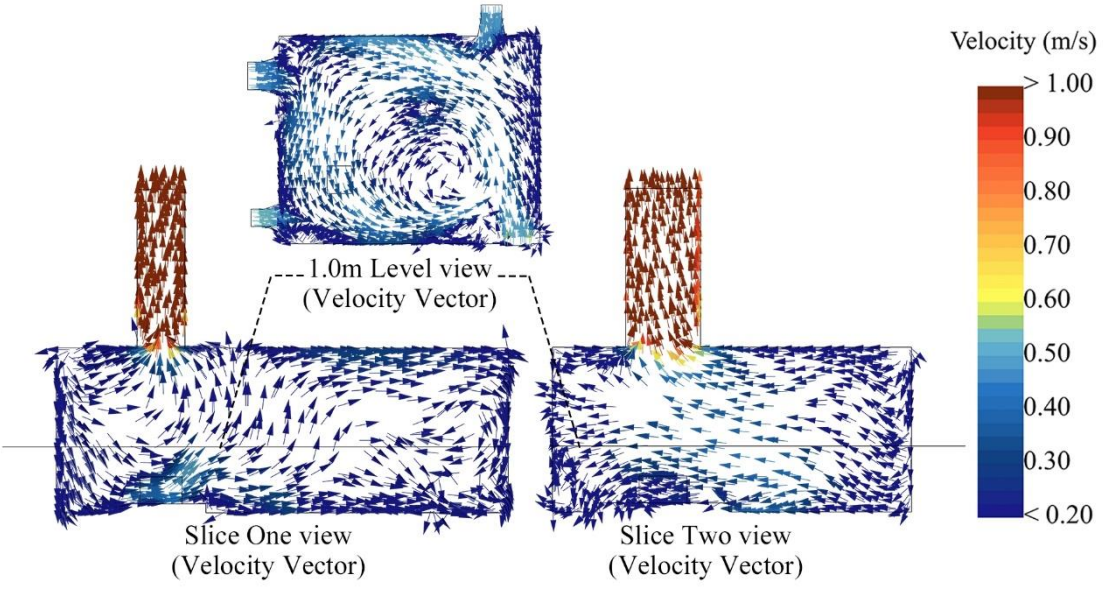

Fig. 7: Vector diagram of indoor flue gas velocity.

Table 6: The instantaneous values of each opening rate and flow rate for stable operating state (‘ + ’ represents outflow, ‘ – ’ represents inflow).

Physical quantity	Inlet 1	Inlet 2	Inlet 3	Inlet 4	Outlet
Sctional area (m^2)	1.28	0.50	0.76	0.42	1.00
Instantaneous velocity of the outlet (m/s)	+0.61	+0.52	+0.44	+0.30	+1.29
Instantaneous flow rate of the outlet (kg/s)	-0.62	-0.22	-0.25	-0.01	+1.09

the indoor carbon dioxide concentration, the changes in various indoor indicators first increase, then decrease, and gradually reach a stable stage. After operating for 300 s, the ACH, SEVR, and the IAT of 1.5 m remain unchanged. The indoor CO_2 concentration fluctuates between 450 ppm and 480 ppm, which can be regarded as reaching a stable state.

(2) Distribution characteristics of flue gas flow velocity: due to the negative pressure effect and buoyancy force of the flue dominating the exhaust path of the flue gas, air enters the room from each door and window opening. Moreover, because the opening area of inlet 1 on the east side is significantly larger than that of other openings, it has an

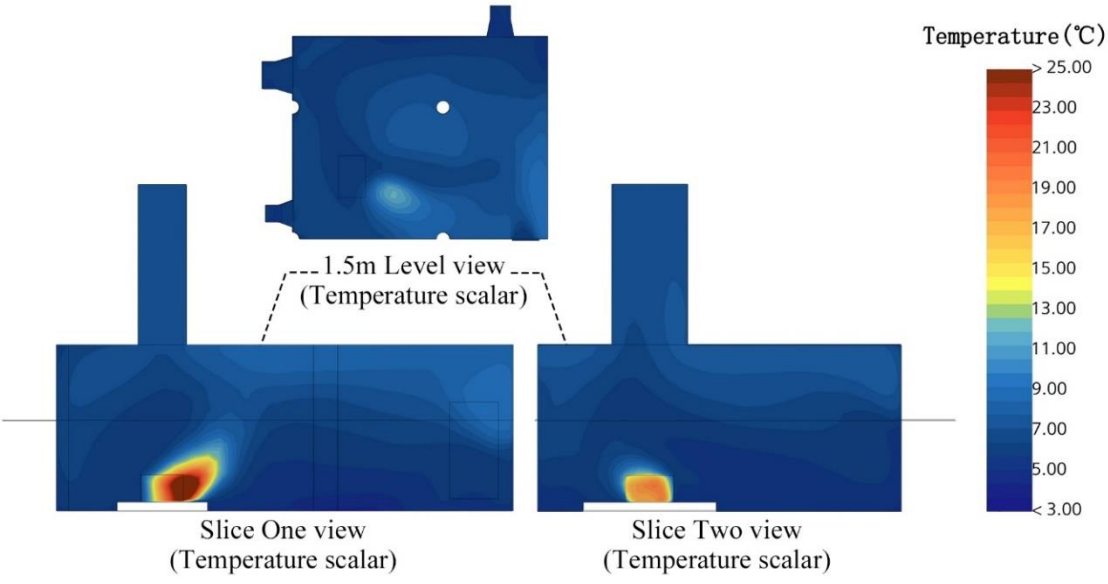

Fig. 8: Indoor sectional temperature chart.

impact on the air intake volume and wind speed at inlet 4 on the west side, forming a vortex at the inlet 4 opening. At some moments, a small amount of air enters inlet 4 and is immediately discharged along the original path. It can be known from Table 6 that after reaching the stable stage, among the flow velocities and flow rates of the four intakes, inlet 1 has the highest flow velocity, which is 0.61 m/s, and the average flow rate entering the room is -0.62 kg/s. The minimum flow velocity of inlet 4 is 0.30 m/s, and the average flow rate entering the room is 0.01 kg/s. Comparing the velocity results of the four openings, Inlet 1 has the highest flow velocity, followed by Inlet 2, Inlet 3, and Inlet 4. In terms of flow rate, Inlet 1 also ranks first, followed by Inlet 3, Inlet 2, and Inlet 4. In Fig. 7, due to the influence of flow velocity, the indoor flue gas diffuses more towards the northeast side where inlet 1 is located. Therefore, a larger opening can allow more fresh air to enter the room. Among the two openings on the south side, inlet 2 is closer to the fire source. Due to the negative pressure effect, its flow velocity is greater than that of inlet 3.

(3) Distribution characteristics of temperature: in Fig. 8, the simulation results indicate that on the horizontal section at a height of 1.5 m close to the personnel activity area, the temperature gradient presents a distribution feature of high center and low edge, and through the efficient smoke exhaust of the flue, the temperature at the center at a height of 1.5 m shows a process of first rising, then falling, and then rising again. It is speculated that before 120 s, due to the enhanced buoyancy force the flue, the temperature decreased. After 120 s, due to the saturation of heat absorption by the wooden wall surface in the flue, the heat loss is reduced, causing the temperature to rise again and reach a stable state. This indicates that the thermal inertia of the wooden chimney has a regulatory effect on the dynamic process of its flue gas flow, and its heat absorption-heat release characteristics lead to a two-stage feature of temperature change. Secondly, due to the strong smoke exhaust capacity of the relay chimney, the peak sectional temperature at 1.5m indoors is only 16.15 ℃, the average sectional temperature at 1.5 m is 7.41 ℃, and the average indoor temperature is 8.33 ℃, which is significantly lower than the conventional thermal comfort standard (ISO 7730 recommends a minimum average indoor temperature of 18.00 ℃ in winter, and the thermal neutral temperature on the Qinghai-Tibet Plateau be 14.5 ℃).[34-36] And it is significantly lower than the expected value of indoor scene heating in the SD.

(4) ACH and comprehensive environmental evaluation: due to the synergistic effect of the relay chimney and the building openings, as well as the parallel opening network formed by the four door and window openings, the air turbulence mixing was intensified. As a result, the calculated ACH during the 900 s dynamic simulation was 35.23 h^{-1}, which was much higher than the specified value of the general ACH (3.00 h^{-1}) in the relevant specifications.[8] It presents an enhanced feature of the exchange of indoor and outdoor air. However, the thermal efficiency of the firepit has decreased, and it may cause smoke to accumulate in the attic space, posing certain fire hazards. It is worth noting that although this ventilation mode poses safety risks, under the exhaust of the large chimney, the indoor smoke can be effectively discharged, and the indoor carbon dioxide concentration meets the specification requirements (less than or equal to 1000 ppm).[8,9]

The design of the large chimney demonstrates the ecological adaptability and wisdom of such buildings to natural ventilation, objectively improving the exhaust efficiency of the smoke, and forming a delicate balance with the residents' demand for fresh air in the high-altitude and low-oxygen environment.

3.2 The influence of chimney section length on indoor air

The variation of the chimney section length (CSL) of the chimney has a significant impact on IAQ as shown in Fig. 9. Specifically:

(1) In terms of ACH, with the increase of the CSL of the chimney, the ACH increased significantly and proportionally, from 15.34 h-1 to 47.78 h-1, and the maximum change rate was 27.53%.

(2) From the perspectives of ICDC, SEVR, and IAT of 1.5 m, all three decreases with the increase of the CSL of the chimney. The variation range of ICDC is from 518.56 ppm to 435.12 ppm, and the maximum change rate was 4.52%. The variation rang e of the average export rate was from 1.41 m/s to 1.26 m/s, and the maximum change rate was only 4.25%. The IAT of 1.5 m is from 8.33 ℃ to 7.21 ℃, and the maximum change rate is 3.10%. This indicates that the sectional size of the chimney mainly affects the flue gas flow rate, and the flue gas flow rate directly affects the ICDC, while having a relatively small influence on the outlet flow velocity and the temperature at a height of 1.5 m.

(3) With the increase of the chimney length, both the ACH and the SEVR show a linear relationship after linear fitting. In terms of ICDC and IAT of 1.5 m, both decrease with the increase of the CSL of the chimney. When the length is less than 0.75 m, the change of the parameters is more sensitive than when the length is greater than 0.75 m. At this time, the CSL of the chimney is 0.60 m^2, slightly larger than the firepit combustion area (0.56 m^2).

3.3 The influence of chimney section width on indoor air

The variation of the chimney sectional width (CSW) of the chimney is more sensitive to the IAQ in some intervals, especially when the width is less than 0.50 m (Seen in Fig. 10). Specifically:

(1) In terms of ACH: with the increase of the CSW, the ACH increases significantly in a direct proportion, from 14.45 h-1 to 47.78 h-1. This indicates that the increase in width can significantly improve the displacement efficiency of indoor air.

(2) Regarding the SEVR: the SEVR decreases inversely with the increase of width, from 1.42 m/s to 1.25 m/s. This indicates that wider chimneys can more effectively reduce the outlet velocity of flue gas and decrease the backflow of flue gas indoors.

(3) In terms of ICDC and IAT of 1.5 m, both decrease with the increase of the CSW of the chimney. When the CSW is less than 0.55 m, the changes in the parameters are more sensitive than when the width is greater than 0.55 m. This indicates that within the range of widths less than 0.55 m, the slight change in width has a greater impact on IAQ. At this time, the chimney area is 0.69 m^2, slightly larger than the firepit combustion area (0.56 m^2). Therefore, considering the regular influence of length variation on flue gas flow, it is suggested that the chimney sectional area be larger than the combustion area of the firepit.

3.4 The influence of chimney section shape on indoor air

This part studies the influence of the chimney sectional shap (CSS) on IAQ. As displayed in Table 7, this paper sets three types of CSS, namely the flat and wide type (length to width ratio 0.64:1), the foundation type (length to width ratio 1.56:1), and the narrow and long type (length to width ratio 4:1). The rate of change of ACH, SEVR, ICDC and IAT of 1.5 m are less than 1.00%. It can be concluded from this that when the sectional area size remains unchanged and the length and width change simultaneously, the change in IAQ is relatively small.

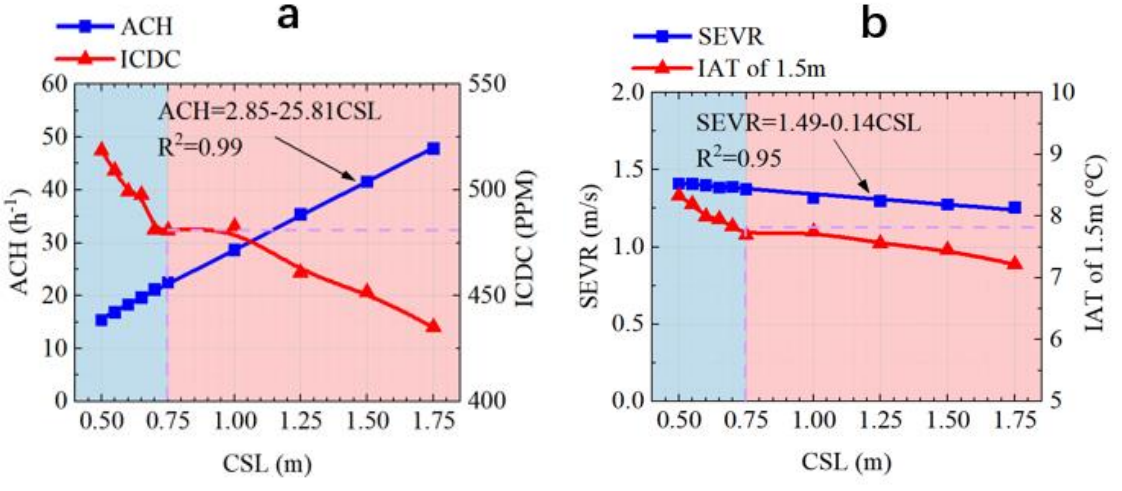

Fig. 9: ACH, ICDC, SEVR, and IAT of 1.5m under different CSL, (a) ACH and ICDC; (b) SEVR and IAT.

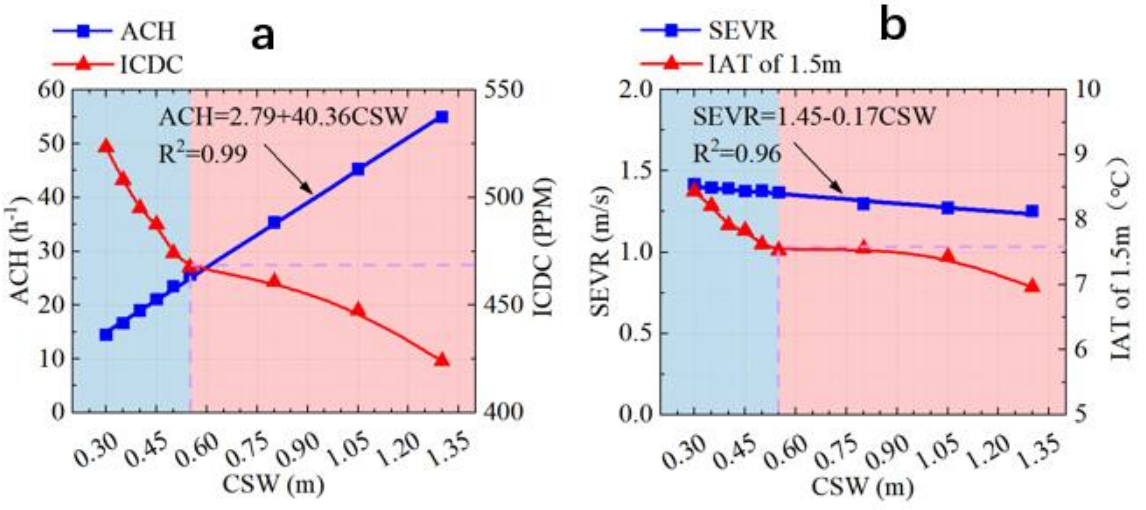

Fig. 10: ACH, ICDC, SEVR, and IAT of 1.5 m under different CSW, (a) ACH and ICDC; (b) SEVR and IAT.

Table 7: Variation of each parameter under different CSS.

CSS	Length-width ratio	Sectional area (m^2)	ACH (h^{-1})	Rate of change (%)	SEVR (m/s)	Rate of change (%)	ICDC (ppm)	Rate of change (%)	IAT of 1.5 m (°C)	Rate of change (%)
Flat and wide chimney	0.64:1	1.00	35.35		1.29		459.54		7.56	
Basic chimney	1.56:1	1.00	35.41	-0.16 (Min)	1.30	-0.56 (Min)	461.94	-0.52 (Min)	7.60	-0.57 (Min)
Long and narrow chimney	4.00:1	1.00	35.36	0.15 (Max)	1.30	0.55 (Max)	460.80	0.52 (Max)	7.55	0.56 (Max)

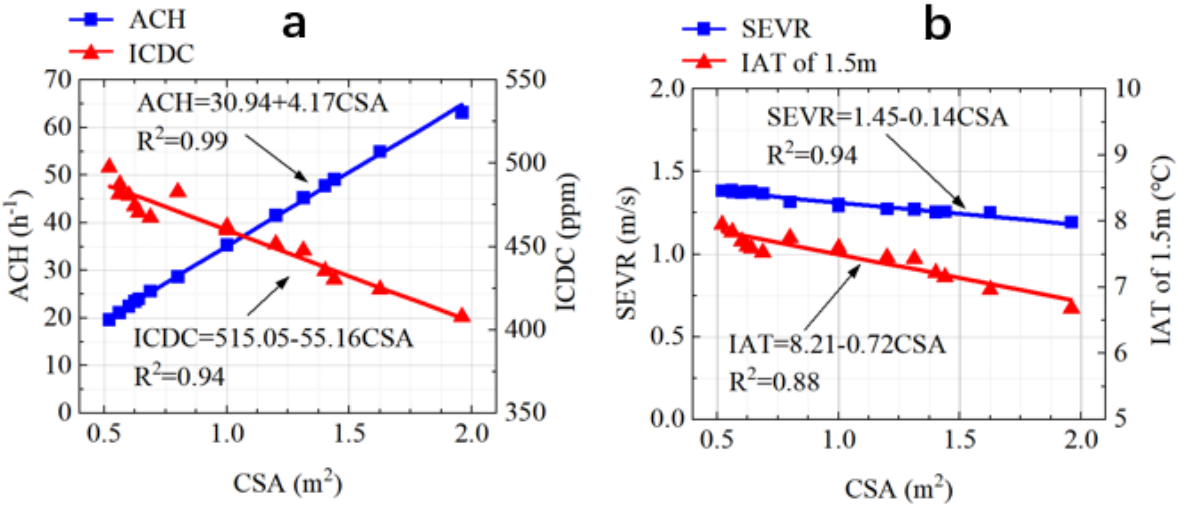

Fig. 11: ACH, ICDC, SEVR, and IAT of 1.5m under different CSA.

3.5 The influence of chimney section area on indoor air

Through the above research, the influence of area changes on IAQ was finally discussed. In Fig. 11, during the process of chimney section area (CSA) increase, all four indicators show a linear change pattern. The ACH increases linearly, while SEVR, ICDC, IAT of 1.5 m all decrease linearly. In conclusion, no matter how the size and shape of the chimney section change, the indoor air flow is actually more related to

the SA and shows a linear change pattern. Furthermore, both ACH and ICDC can meet the specification requirements (ACH is much greater than 3.00 h^{-1}, and ICDC is much less than 1000 ppm),[8] which proves the effectiveness of these chimneys in controlling smoke emissions.

4. Conclusion

In this study, through numerical simulation methods, a case of a certain SD in northwest Yunnan was selected as the research object, and the indoor flue gas flow characteristics of the SD under different chimney design parameters and their influence on air quality are systematically analyzed. Results show that the increase in the sectional size of the chimney can significantly improve the ACH, and reduce the soot density and indoor temperature, thereby improving the IAQ. The specific conclusions are as follows:

(1) During the process of chimney section change, the influence of length and width (single-factor variables) on the indoor air flow are the same. When it is less than the critical point, the influence brought by the change is more sensitive (chimney section length less than 0.75 m, chimney section width less than 0.55 m). When the length and width change simultaneously, regardless of whether the length-to-width ratio remains unchanged or not, the overall law changes linearly, that is, the indoor flue gas flow law changes linearly under the influence of the sectional area of the chimney.

(2) The change in the shape of the chimney has a relatively small impact on the indoor flue gas flow situation. The rate of change of ACH, SEVR, ICDC, and IAT of 1.5 m are less than 1.00%. Therefore, the sectional shape of the chimney has a relatively small impact on the IAQ.

(3) When the chimney sectional area of the chimney is larger than that of the firepit combustion area, the change rates of various IAQ indicators are all lower than the situation where the sectional area of the chimney is smaller than that of the firepit combustion area. This indicates that the indoor air exchange volume is sufficient to meet the emission requirements of soot at this time. When the sectional size of the chimney is further increased, the sensitivity of the parameters to its influence decreases. Therefore, in practical applications, it is recommended that the chimney size be applications, it is recommended that the chimney size be slightly larger than the firepit size to optimize IAQ.

This research not only provides a scientific basis for the design of the relay smoke exhaust system of the SD, but also is of great significance for improving IAQ and ensuring the health of residents. By quantifying the influence of different chimney sizes on indoor flue gas flow and air quality, the flow and influence laws were summarized, providing specific guidance for the modernization transformation and optimization of traditional buildings and helping to reduce health problems caused by indoor fire use.

Acknowledgements

The authors acknowledge Tianfu Yongxing Laboratory and China-Portugal Joint Laboratory of Cultural Heritage Conservation Science supported by the Belt and Road Initiative. This research was financially supported by the National Key R&D Program of China (grant No. 2024YFC3808300), the National Natural Science Foundation of China (grant No. 52408136), the WeizhouTeam Funds in Southwest Minzu University (grant No. SMUWZ202408) and the Sichuan Provincial Youth Scientific and Technological Innovation Research Team on Ecological Adaptability of Plateau Architecture (grant No. 2022JDTD0008).

Conflict of Interest

There is no conflict of interest.

Supporting Information

Applicable.

CRediT Statement

Yunke Yang: Writing – Original draft, Project administration, Investigation, Software, Data curation. **Xiaoliang Wang:** Writing –review & editing, Supervision, Methodology, Formal analysis, Investigation. **Guanxing Pu:** Writing – review & editing, Supervision, Investigation. **Junjia Hu:** Supervision, Investigation. **Shuliang Li:** Supervision, Resources, Project administration. **Li Yang:** Supervision, Resources, Project administration. **Xianmin Mai:** Review, Supervision, Resources, Funding acquisition.

References

[1] H. Y. Zhang, The ecological mode and contemporary design application of traditional Tibetan houses in Diqing, Xi'an University of Architecture and Technology, 2020, doi: 10.27393/d.cnki.gxazu.2020.001457.

[2] X. Liu, G. Shen, L. Chen, Z. Qian, N. Zhang, Y. Chen, Y. Chen, J. Cao, H. Cheng, W. Du, B. Li, G. Li, Y. Li, X. Liang, M. Liu, H. Lu, Z. Luo, Y. Ren, Y. Zhang, D. Zhu, S. Tao, Spatially resolved emission factors to reduce uncertainties in air pollutant emission estimates from the residential sector, *Environmental Science & Technology*, 2021, **55**, 4483-4493, doi: 10.1021/acs.est.0c08568.

[3] S. Li, X. Liu, J. Wang, J. Li, Z. Wang, S. Ma, Z. Dong, M. Li, Y. Han, J. Cao, Exposure to polycyclic aromatic hydrocarbons (PAHs) from domestic heating and cooking combustion of different fuel types for Elders in rural China, *Environmental Pollution*, 2024, **357**, 124416, doi: 10.1016/j.envpol.2024.124416.

[4] W. Du, J. Wang, S. Zhang, N. Fu, F. Yang, G. Wang, Z. Wang, K. Mao, G. Shen, M. Qi, S. Liu, C. Wu, Y. Chen, Impacts of Chinese spring festival on household $PM_{2.5}$ pollution and blood pressure of rural residents, *Indoor Air*, 2021, **31**, 1072-1083, doi: 10.1111/ina.12795.

[5] R. Jin, M. Zheng, L. Yang, G. Lammel, X. Zhou, Y. Sun, C. Chen, B. Lin, G. Liu, Model evaluation of indoor exposure to polychlorinated dibenzo-p-dioxins and dibenzofurans and polycyclic aromatic hydrocarbons from household fuel combustion in rural areas of Tibetan Plateau, *Exposure and*

Health, 2023, **15**, 145-159, doi: 10.1007/s12403-022-00482-4.
[6] J. Zhang, K. R. Smith, Household air pollution from coal and biomass fuels in China: measurements, health impacts, and interventions, *Environmental Health Perspectives*, 2007, **115**, 848-855, doi: 10.1289/ehp.9479.
[7] X. Zhang, C. P. Barrington-Leigh, B. E. Robinson, Rural household energy transition in China: trends and challenges, *Journal of Cleaner Production*, 2024, **450**, 141871, doi: 10.1016/j.jclepro.2024.141871.
[8] China Architecture and Building Press, Design code for heating ventilation and air conditioning of civil buildings, Beijing, 2012.
[9] China Standards Press, Standards for indoor air quality, Beijing, 2022.
[10] L. Tian, D. Lucas, S. L. Fischer, S. C. Lee, S. K. Hammond, C. P. Koshland, Particle and gas emissions from a simulated coal-burning household fire pit, *Environmental Science & Technology*, 2008, **42**, 2503-2508, doi: 10.1021/es0716610.
[11] N. R. Martins, G. Carrilho da Graça, Health effects of $PM_{2.5}$ emissions from woodstoves and fireplaces in living spaces, *Journal of Building Engineering*, 2023, **79**, 107848, doi: 10.1016/j.jobe.2023.107848.
[12] M. Shan, D. K. Li, X. D. Yang, Study on Influences of Combustion of Fire Place on Indoor Environment and Thermal Comfort in Rural Residences, *Building Science*, 2011, **27**, 10-14, doi: 10.13614/j.cnki.11-1962/tu.2011.06.006.
[13] H. L. Liu, Z. J. Yang, M. F. Tang, Field Study on Indoor Thermal Environment of Zhuang Traditional Dwellings in Northwest Guangxi in Winter, *Building Science*, 2021, **37**, 113-121, doi: 10.13614/j.cnki.11-1962/tu.2021.06.15.
[14] Y. T. Zhang, B. Che, Y. J. Zhang, Simulation study on the law of fire smoke propagation under the stack effect, J*ournal of Safety and Environment*, 2023, **23**, 740-748, doi: 10.13637/j.issn.1009-6094.2021.1777.
[15] H. Cui, J. Chen, Z. Dong, Z. Han, Q. Liu, Numerical study of the fire-smoke temperature law in the shaft of a high-rise building under the chimney effect in winter, *Engineering Applications of Computational Fluid Mechanics*, 2023, **17**, 2222811, doi: 10.1080/19942060.2023.2222811.
[16] R. A. Rohde, R. A. Muller, Air pollution in China: mapping of concentrations and sources, *PLoS One*, 2015, **10**, e0135749, doi: 10.1371/journal.pone.0135749.
[17] M. Cheng, D. Jiang, C. Zhang, The Control Strategy of Pollutant Release from Traditional Residential Fireplaces in Western Hu'nan: A Case Study of Laodong Village, Fenghuang County, *Huazhong Architecture*, 2022, **40**, 35-39, doi: 10.13942/j.cnki.hzjz.2022.02.002.
[18] F. Zhang, L. Shi, S. Liu, J. Shi, M. Cheng, Indoor air quality in Tujia dwellings in Hunan, China: field tests, numerical simulations, and mitigation strategies, *International Journal of Environmental Research and Public Health*, 2022, **19**, 8396, doi: 10.3390/ijerph19148396.
[19] M. A. Johnson, C. R. Garland, K. Jagoe, R. Edwards, J. Ndemere, C. Weyant, A. Patel, J. Kithinji, E. Wasirwa, T. Nguyen, D. D. Khoi, E. Kay, P. Scott, R. Nguyen, M. Yagnaraman, J. Mitchell, E. Derby, R. A. Chiang, D. Pennise, In-home emissions performance of cookstoves in Asia and Africa, *Atmosphere*, 2019, **10**, 290, doi: 10.3390/atmos10050290.
[20] F. Wang, X. Liu, P. Liang, Study on winter's indoor thermal environment of dong minority's pile dwellings in southeast of Guizhou province under natural ventilation, *Interior Design + Construction*, 2023, **8**, 124-125, doi: 10.3969/j.issn.1005-7374.2023.08.028.
[21] L. Li, Indoor Thermal Environment of Tibetan Folk Houses with Rammed-earth Wall in Xiaozhongdian, Shangri-la, *Huazhong Architecture*, 2009, **27**, 271-274, doi: 10.3969/j.issn.1003-739X.2009.03.062.
[22] M. L. Duan, Y. Zhao, Z. S. Wang, H. W. Shu, J. L. Zhu, H. N. Shan, Research and Assessment Method of Thermal Performance of Chinese Kang, *Building Science*, 2009, **25**, 30-38, doi: 10.3969/j.issn.1002-8528.2009.12.007.
[23] D. Wang, C. Z. Xu, G. W. Li, H. B. Cai, Simulation study on the technology for improving the temperature distribution of Kang surface, *Journal of Harbin Institute of Technology*, 2012, **44**, 75-79, doi:10.11918/j.issn.0367-6234.2012.04.016.
[24] Q. Zhang, Flue gas flow and thermal performance of kangs in northeast traditional dwellings, Harbin Institute of Technology, 2017, doi: 10.7666/d. D01332908.
[25] J. Zhang, L. Z. Chen, Y. Xue, Thermal comfort of large complexity kang based on improving kang hole structural form, *Science Technology and Engineering*, 2019, **19**, 262-267, doi: 10.3969/j.issn.1671-1815.2019.08.041.
[26] J. Zhang, L. Z. Chen, W. D. Wang, Flue form optimization design of large complexity kang based on temperature field simulation, *Transactions of the Chinese Society of Agricultural Engineering*, 2019, **35**, 233-239, doi: 10.11975/j.issn.1002-6819.2019.17.028.
[27] L. Z. Chen, Study on the Optimization Design of Large Complexity Kang Flue Structure aiming at lmproving Thermal Comfort and Thermal Efficiency, Inner Mongolia University of Science & Technology, 2019, doi: 10.27724/d.cnki.gnmgk.2019.000213.
[28] H. Q. Li, M. D. Bi, X. H. Yang, L. F. Liu, Y. Zhou, F. Xu, G. Q. Zhang, Research on Heterogeneous Design and Performance Optimization of Chinese Traditional Heated Kang, *Journal of Hunan University (Natural Sciences)*, 2023, **50**, 165-175, doi: 10.16339/j.cnki.hdxbzkb.2023112.
[29] Y. H. An, X. Y. Ma, A. Q. Wang, L. L. Xu, Simulation Analysis of Indoor Air Distribution in Existing Natatorium Based on Natural Ventilation, *Journal of Shenyang Jianzhu University (Natural Science)*, 2024, **40**, 148-15, doi: 10.11717/j.issn:2095-1922.2024.01.17.
[30] K. Y. Wang, Z. Z. Zhen, M. J. Chen, H. Q. Yao, X. Liu, W. K. Zhang, Investigation on the Natural Ventilation Scheme of Office Based on the CFD Simulation, *Journal of BEE*, 2023, **51**, 102-108, doi: 10.3969/j.issn.2096-9422.2023.12.017.
[31] Siemens Digital Industries Software, STAR-CCM+ User Guide (Version 2306), Plano, Texas, 2023.
[32] China Architecture & Building Press, Code for Thermal Design of Civil Building, Beijing, 2016

[33] Y. X. Zhu, Chapter 6 (Theoretical basis for creating an indoor air environment), Building Environment (3rd Edition), *China Architecture & Building Press*, Beijing, 2010, 223-224, ISBN: 978-7112116992.
[34] International Organization for Standardization, Ergonomics of the thermal environment - Analytical determination and interpretation of thermal comfort using calculation of the PMV and PPD indices and local thermal comfort criteria, Geneva, 2005.
[35] Y. Han, X. Wang, L. Lu, X. Mai, Adaptive thermal sensation evaluation model in tents for Western Sichuan Plateau of China: a field study, *Energy and Buildings*, 2023, **286**, 112952, doi: 10.1016/j.enbuild.2023.112952.
[36] L. Lu, T. Zhang, X. Wang, Y. Han, D. Sridhar, H. Li, B. B. Xu, K. V. Fedorovich, X. Mai, Evaluation and analysis of the architectural environment of traditional folk houses in Tibetan Plateau, China, *Engineered Science*, 2023, **22**, 845, doi: 10.30919/es8d845.